

Theoretical Study on Relationship Between Structure of Mercapto-Triazole Derivatives and Inhibition Performance

Shuangkou Chen^{1,*}, Steve Scheiner², Tapas Kar², Upendra Adhikari²

¹ College of Chemistry and Chem-engineering, Chongqing University of Science and Technology, Chongqing 401331, China;

² Department of Chemistry and Biochemistry, Utah State University, Logan, UT 84322-0300, USA

*E-mail: cskcn@yeah.net

Received: 25 June 2012 / Accepted: 17 July 2012 / Published: 1 August 2012

Relationships between corrosion inhibition efficiency of five kinds of mercapto-triazole inhibitors and their molecular electronic properties have been theoretically studied at the level of DFT/B3LYP with 6-31+G (d, p) base sets. Calculation results are discussed using linear regression analysis to determine the most effective parameters to establish inhibition efficiency. Regression equations find inhibition performances have a good linear relationship with E_{HOMO} and $(E_{HOMO} - E_{LUMO})$. The adsorption energies are well accorded with the reported experimental results. Finally, this research may provide a theoretical inhibition performance prediction approach for new homologous inhibitors.

Keywords: modeling studies; corrosion inhibition; Schiff base; inhibition performance prediction

1. INTRODUCTION

The inhibition of corrosion of metal and metal alloys is an important goal, and one which is widely practiced in the petroleum, chemical, and construction industries. Unfortunately, many currently used corrosion inhibitors contain harmful ingredients [1]. Recent research has thus given high priority to developing new, efficient, and environmentally friendly corrosion inhibitors [2,3]. Multi-unit triazole compounds (polycell triazole compounds) are stimulating growing attention owing to their special molecular structure and good corrosion inhibition performance [4,5]. Some relevant theoretical and experimental studies have been carried out [6,7,8,9,10,11], some of which considered possible correlation of the inhibition efficiency with calculated quantum chemical parameters, such as E_{HOMO} , E_{LUMO} , and $\Delta E (E_{HOMO} - E_{LUMO})$ to seek links between them. (E_{HOMO} and E_{LUMO} refer to the energy of Highest Occupied and Lowest Unoccupied Molecular Orbital, respectively). These theoretical

calculations accorded well with the experimental results. Quraishi et al. [12,13] and Bentiss et al. [14] designed and synthesized a series of multi-unit triazole compounds (polycell triazole compounds) and carried out a series of studies on their corrosion inhibition performance, finding that a sulfhydryl triazole compound has the advantage of adapting itself in a wide range of acidic solution and broad temperature range and is environmentally friendly.

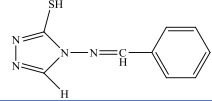
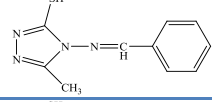
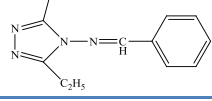
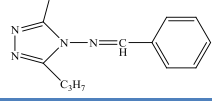
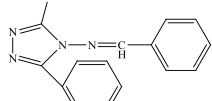
Quantum chemical methods have proven themselves an effective research tool when applied to the structure and performance of corrosion inhibitors, facilitating the design of new agents [15]. These methods have provided specific information about molecular structure, electron distribution and adsorption processes of corrosion inhibitors. They are also beneficial for understanding the relationship between the structure and performance of corrosion inhibitors, and for studying corrosion inhibition at the microscopic level. If some relationships between molecular structure and their properties can be found, other new kinds of inhibitors could be screened by using quantum calculation methods which will guide a new series of computer simulations [11,16] and molecular design [17] for new corrosion inhibitors.

The study of Khaled [18] represents a good example of how one might screen and evaluate several different triazole molecules, documenting the importance of a high E_{HOMO} and low dipole moment. Duda et al. [19] investigated and developed a strategic algorithm to design new imidazoline-type compounds using computer simulations by calculating their theoretical partition coefficients and molecular volumes. These two indices were correlated with inhibition efficiency.

Many papers have reported that, in order to obtain a good inhibition effect, the inhibitors should contain certain functional groups [20,21,22] such as nitrogen, oxygen, and sulphur [23,24,25], which could help to donate electrons. Usually the inhibitors contain some rings [20,25,26,27,28] that might allow extraction of electrons and have the ability to adsorb on a metal surface [21,26], and then form a physical or chemical film to protect the metal from corrosion, which may be a general mechanism for the inhibitors [29,30]. Typically, the corrosion inhibitor performance is related to its ability to donate electrons. In general, electron donating ability of a molecule is associated with E_{HOMO} , with a high value of E_{HOMO} revealing a strong tendency of the molecule to donate electrons to other possible acceptor molecules with empty low energy molecular orbitals. As for metal surfaces, the metal atoms often have empty orbitals facilitating their ability to accept electrons from donors (inhibitors).

One of the more recently developed types of corrosion inhibitors that is enjoying some success are those pictured in Table 1. Each such molecule is characterized by the presence of a phenyl ring and a five-membered heteroatomic aromatic system, conjoined by an imine CH=N group. It is hoped to build on this success, to provide an improved theoretical inhibition performance evaluation approach for homologous inhibitors, so as to design and predict performance for new homologous inhibitors. The current work is designed for that purpose. The five molecules pictured in Table 1 are taken as a test bed, since there are data available regarding the effectiveness of each. By applying quantum calculations, it is our goal first to identify those aspects of this class of molecules that are intrinsic to their activity. Having done so, we propose modifications on the template that might improve their effectiveness.

Table 1. Abbreviations and molecular structures of the studied compounds.

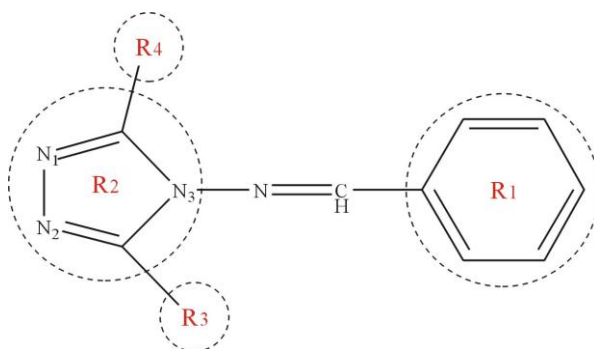
Inhibitor	Conformation	Abbreviation
4-aminobenzylidene-5-mercapto-1,2,4-triazolez(ABMT)		A1
3-methyl-4-aminobenzylidene-5-mercapto-1, 2, 4-triazole (MABMT)		B1
3-ethyl-4-aminobenzylidene-5-mercapto-1,2,4-triazole(EABMT)		C1
3-propyl-4-aminobenzylidene-5-mercapto-1,2,4-triazole(PABMT)		D1
3-phenyl-4-aminobenzylidene-5-mercapto-1,2,4-triazole (PhABMT)		E1

2. CALCULATION METHOD

Density Functional Theory (DFT) [31,32] which is an economic and efficient quantum chemistry computing method can provide accurate information about geometrical configuration and electron distribution. DFT is widely applied in the analysis of corrosion inhibition performance and the interaction of corrosion inhibitors and interfaces [3,26,27]. The B3LYP functional was applied within the context of Gaussian 09 [33], using the 6-31+G(d, p) basis set [34,35]. Optimized structures were verified as minima via the presence of all positive harmonic frequencies. In the aqueous phase calculations, the theoretical model was considered via SMD, using a dielectric constant of 78.5 for water [36]. Frequency analysis showed there was no imaginary frequency, indicating that the calculated geometry represented a stable minimum on the potential energy surface. We also studied the interaction of inhibitor molecules with a Fe surface by using the molecular dynamics method [26]. The iron surface was modeled by two adjacent layers. The system was optimized by the smart minimizer method with T=298K.

3. RESULTS AND DISCUSSION

The atomic numbering scheme is presented in Fig 1, where R1 represents the indicated phenyl ring, R2 the triazole ring, and R3 and R4 are various substituents added to the latter. The calculated energies of the HOMO and LUMO of each molecule are reported in Table 2, along with atomic and group charges, computed via the Mulliken procedure. ΔE is used to indicate the difference in energy between the HOMO and LUMO. The last column displays the experimentally derived corrosion inhibition efficiency [37,38].



$R_3 = \text{H}$ (A1), $-\text{CH}_3$ (B1), $-\text{C}_2\text{H}_5$ (C1), $-\text{C}_3\text{H}_7$ (D1), $-\text{Ph}$ (E1), $R_4 = -\text{SH}$

Figure 1. The molecular schematic of inhibitor

Table 2. Quantum chemical parameters of the studied inhibitors calculated at B3LYP/6-31+G (d, p) level.

Phase ^a	Inhibitor	E_{HOMO} (eV)	E_{LUMO} (eV)	ΔE^b (eV)	Q_{N1}	Q_{N2}	Q_{N3}	Q_{R1}	Q_{R2}	Q_{R3}	Q_{R4}	$Q_{(\text{R2}+\text{R3})}$	$Q_{(\text{R2}+\text{R3}+\text{R4})}$	η^c
G	A1	-6.599	-2.626	-3.973	-0.180	-0.168	-0.129	0.285	-0.423	0.000	0.250	-0.423	-0.173	91.43
	B1	-6.365	-2.530	-3.835	-0.209	-0.072	-0.192	0.142	-0.114	-0.670	0.209	-0.784	-0.575	92.63
	C1	-6.316	-2.529	-3.787	-0.227	-0.055	-0.176	0.126	-0.463	-0.615	0.211	-1.078	-0.867	95.53
	D1	-6.300	-2.520	-3.780	-0.226	-0.032	-0.155	0.119	-1.063	-0.316	0.196	-1.379	-1.183	96.47
	E1	-6.235	-2.561	-3.674	-0.237	-0.027	-0.110	0.114	-0.309	-0.663	0.244	-0.972	-0.728	97.48
A	A1	-6.642	-2.164	-4.478	-0.219	-0.290	-0.142	-0.977	-0.636	0.000	0.188	-0.636	-0.448	91.43
	B1	-6.529	-2.103	-4.426	-0.321	-0.233	-0.176	0.044	-0.298	-0.695	0.163	-0.993	-0.830	92.63
	C1	-6.502	-2.117	-4.385	-0.333	-0.212	-0.174	0.079	-0.676	-0.619	0.168	-1.295	-1.127	95.53
	D1	-6.494	-2.118	-4.377	-0.333	-0.197	-0.154	0.039	-1.244	-0.368	0.156	-1.612	-1.456	96.47
	E1	-6.431	-2.178	-4.253	-0.379	-0.099	0.013	-0.198	-0.314	-0.845	0.203	-1.159	-0.956	97.48

^a G, gas phase (dielectric constant $\epsilon = 1.0$); A, aqueous phase (dielectric constant $\epsilon = 78.5$). ^b $\Delta E = E_{\text{HOMO}} - E_{\text{LUMO}}$. ^c Exp. value from Ref. [37,38], the inhibiting effect efficiency (η) for the corrosion of the mild steel in 1.0 M HCl with addition of 0.4 g L⁻¹ of various inhibitors at 298K on the basis of electrochemical measurements [37].

3.1. Frontier molecular orbital characteristic of corrosion inhibitor

The three-dimensional extents of the HOMO and LUMO of each species are illustrated in Fig.2, from which it may be noted that there is strong similarity from one molecule to the next. The HOMO is largely localized on the triazole ring and its substituents, whereas the LUMO is spread more evenly over the entire molecule, with greater emphasis on the phenyl ring. If the corrosion resistance were due primarily to a transfer of charge from the HOMO to the metal surface, then one might anticipate greater involvement of the triazole region. The opposite trend of phenyl ring participation would result from charge transfer from the surface to the inhibitor LUMO.

Both unitary and linear fitting of the HOMO and LUMO energies against the corrosion inhibition efficiency η lead to the parameters displayed in Table 3. The best correlation is observed with the HOMO-LUMO energy difference, with the HOMO energy not far behind. Indeed, the latter is the best correlated with the experimental quantity in aqueous phase. One might infer that higher HOMO energy facilitates charge extraction to the surface and ultimately to corrosion resistance.

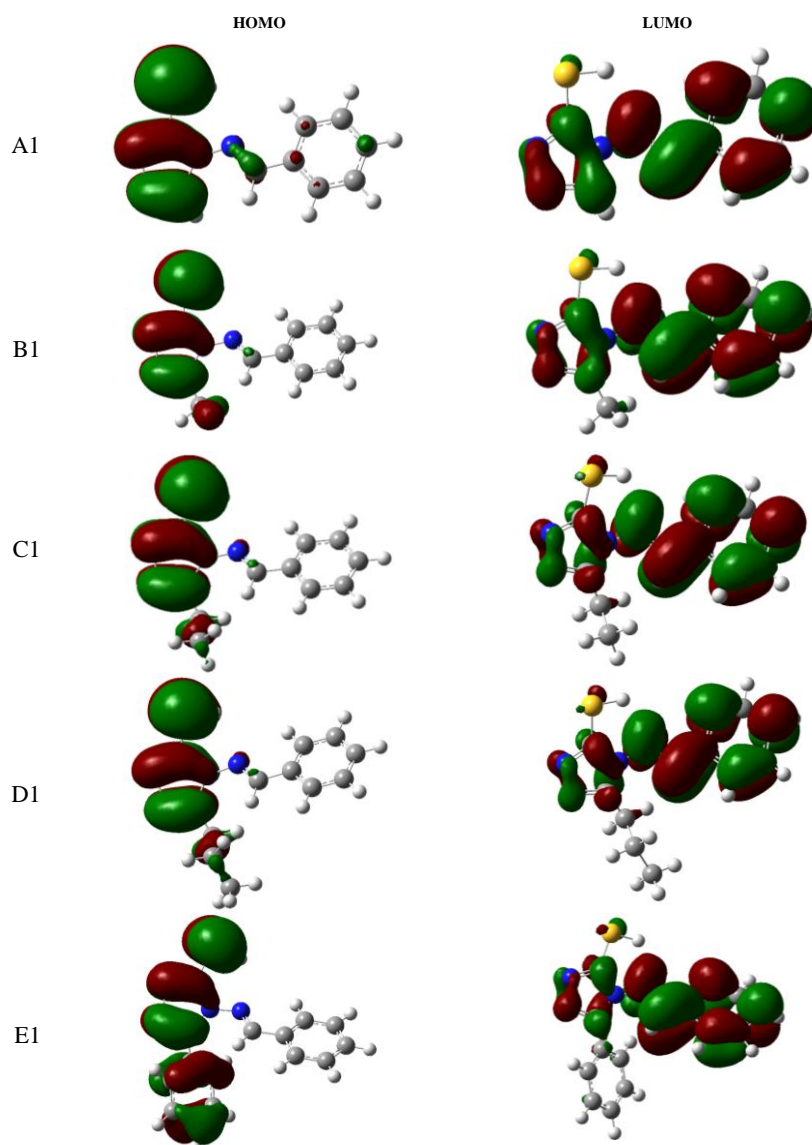


Figure 2. HOMO and LUMO isosurfaces with a value of 0.02a.u. for inhibitors A1, B1, C1, D1 and E1

Table 3. The regression equations of corrosion inhibition efficiency and their frontier orbital energy

Phase ^a	Variable	regression equation		Multiple R	R Square	SE
G	E_{HOMO}	$\eta=199.049+16.398* E_{HOMO}$	(1)	0.890	0.792	1.356
	E_{LUMO}	$\eta=177.848+32.564* E_{LUMO}$	(2)	0.551	0.303	2.482
	$E_{HOMO} \setminus E_{LUMO}$	$\eta=174.339+22.669* E_{HOMO} -25.307* E_{LUMO}$	(3)	0.927	0.860	1.365
	ΔE	$\eta=178.556+22.008*\Delta E$	(4)	0.926	0.858	1.119
A	E_{HOMO}	$\eta=292.769+30.379* E_{HOMO}$	(5)	0.912	0.831	1.221
	E_{LUMO}	$\eta=72.248-10.516* E_{LUMO}$	(6)	0.135	0.018	2.947
	$E_{HOMO} \setminus E_{LUMO}$	$\eta=268.305+30.462* E_{HOMO} -11.708* E_{LUMO}$	(7)	0.924	0.854	1.392
	ΔE	$\eta=215.951+27.657*\Delta E$	(8)	0.897	0.805	1.315

^a G, gas phase (dielectric constant $\epsilon = 1.0$); A, aqueous phase (dielectric constant $\epsilon = 78.5$)

3.2. Correlation between charge and inhibition performance

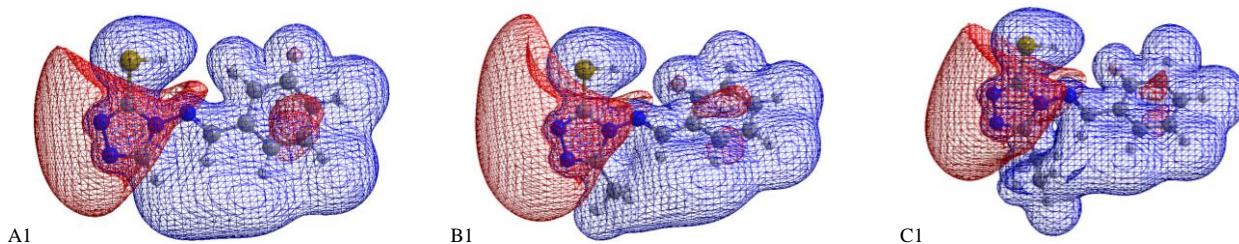
Table 4. The regression equations of Corrosion inhibition efficiency and different net charges

Phase ^a	Variable	regression equation		R/Multiple R	R ² /R Square	SE
G	Q _{N1}	$\eta=71.327-108.346* Q_{N1}$	(9)	0.942	0.888	0.995
	Q _{N2}	$\eta=97.534+39.922* Q_{N2}$	(10)	0.888	0.788	1.368
	Q _{N3}	$\eta= 98.083+22.142* Q_{N3}$	(11)	0.288	0.083	2.848
	Q _{R1}	$\eta=99.229-28.762* Q_{R1}$	(12)	0.807	0.651	1.758
	Q _{R2}	$\eta=93.315-2.935* Q_{R2}$	(13)	0.406	0.165	2.718
	Q _{R3}	$\eta=92.708-4.417* Q_{R3}$	(14)	0.501	0.251	2.573
	Q _{R4}	$\eta=100.535-26.249* Q_{R4}$	(15)	0.241	0.058	2.886
	(Q _{R2} +Q _{R3})	$\eta=89.195-5.946*(Q_{R2}+Q_{R3})$	(16)	0.819	0.671	1.705
	(Q _{R2} +Q _{R3} +Q _{R4})	$\eta=90.830-5.499*(Q_{R2}+Q_{R3}+Q_{R4})$	(17)	0.796	0.633	1.802
	A	Q _{N1}	$\eta=82.774-37.646* Q_{N1}$	(18)	0.864	0.747
Q _{N2}		$\eta=101.517+33.021* Q_{N2}$	(19)	0.892	0.795	1.345
Q _{N3}		$\eta=96.986+17.997* Q_{N3}$	(20)	0.554	0.307	2.475
Q _{R1}		$\eta=95.392+3.378* Q_{R1}$	(21)	0.586	0.343	2.410
Q _{R2}		$\eta=93.725-1.551* Q_{R2}$	(22)	0.231	0.053	2.893
Q _{R3}		$\eta=92.339-4.687* Q_{R3}$	(23)	0.603	0.363	2.373
Q _{R4}		$\eta=92.292+13.756* Q_{R4}$	(24)	0.104	0.011	2.958
(Q _{R2} +Q _{R3})		$\eta=88.239-5.680*(Q_{R2}+Q_{R3})$	(25)	0.797	0.636	1.795
(Q _{R2} +Q _{R3} +Q _{R4})		$\eta=89.570-5.333*(Q_{R2}+Q_{R3}+Q_{R4})$	(26)	0.770	0.593	1.898

^a G, gas phase (dielectric constant $\epsilon = 1.0$); A, aqueous phase (dielectric constant $\epsilon = 78.5$)

Correlations were also sought between the experimental corrosion inhibition parameter and the charges of various atoms and groups. The charge of N₁ correlates best, with R=0.94; N₂ is also found to correlate well (R=0.89). These correlations are modestly improved in the aqueous phase. Within the context of groups, R₁ seems to do best, with R=0.81. This observation is perhaps at odds with the HOMO energy correlation as this orbital is not centered on the R₁ ring. On the other hand, the sum of the R₂ + R₃ charges does correlate rather well with η , even better than R₁, which reinforces the importance of the HOMO.

In addition to charge transfer, one might also inquire about simple electrostatic interactions that might influence the ability of the inhibitor to interact with the metal surface. The molecular electrostatic potential surface for each molecule is presented in Fig.3 where it may be noted that the potential surrounding the triazole ring R₂ is negative, in contrast to the positive potential surrounding the phenyl portion of each molecule.



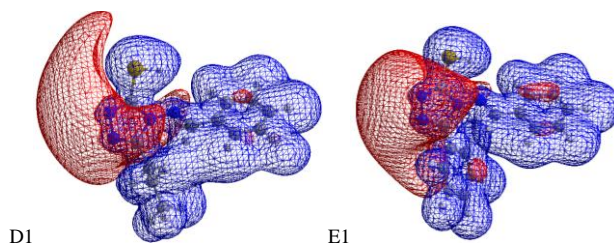


Figure 3. Molecular electrostatic potential surfaces for inhibitors with isopotential value of ± 0.8 au. Negative regions are shown in red, positive in blue

3.3. Interaction between Inhibitors and Fe (100) surface

A Fe (100) surface, modeled by clusters of Fe₅₀ (30, 20), was chosen for molecular mechanics calculations. The Fe(100) surface was first optimized to minimum energy, and then the inhibitor molecule was added on the surface. The simulation used a CVFF force field [39] with T=298 K, NVT ensemble, with a time step of 1.0 fs and simulation time of 100.0 ps. The adsorption energy of each inhibitor molecule on the Fe₅₀ (30, 20) cluster was calculated by the following expression [40]:

$$E_{ads} = E_{\text{molecule/surface}} - (E_{\text{molecule}} + E_{\text{surface}})$$

E_{ads} refers to adsorption energy, E_{molecule} is the energy of the free molecule, and E_{surface} refers to the energy of the metal surface. $E_{\text{molecule/surface}}$ is the total energy of the inhibitor molecule adsorbed on the metal surface. Negative value of E_{ads} is associated with favorable adsorption energy while positive values indicate a repulsive interaction.

Table 5. Statistic average values of adsorption energies (E_{ads}), and distances (d) on iron surface for inhibitors

Molecule	$E_{ads}/(\text{kcal}\cdot\text{mol}^{-1})$	d/Å	η
A1	-164.94	2.791	91.43
B1	-177.24	2.734	92.63
C1	-197.84	2.856	95.53
D1	-207.77	2.959	96.47
E1	-225.12	2.812	97.48

After simulation the results show that, regardless of the original structure chosen, either parallel or perpendicular to the surface, a parallel alignment is preferred. Table 5 reports the statistical average values of adsorption energies (E_{ads}) and the distances (d) separating the inhibitor from the iron surface. All adsorption energies are negative, indicating that all the five inhibitor molecules can effectively adsorb on metal surface. Inhibitor A1 is connected with the smallest adsorption energy, -164.94 kcal \cdot mol⁻¹; and Inhibitor E1 the largest, -225.12 kcal \cdot mol⁻¹. Inhibitor E1 is special in structure as it contains numerous action centers, such as the triazole ring, two benzene rings, and a sulfhydryl which can effectively improve the adsorption capacity on the metal surface and easily form an adsorptive protective film. From the adsorption energies, the corresponding inhibition efficiency are also increasing as the following order of A1<B1<C1<D1<E1. This result is accorded with former analysis via quantum chemical method, and also is well accorded with the reported experimental

results.

3.4. Prediction of the efficiency of some new inhibitors

Table 6. Eight groups of homologous structure of inhibitors

Group	R1	R2	R3	R4
Group 1*	-Ph	Triazole	-H (A1), -CH ₃ (B1), -C ₂ H ₅ (C1), -C ₃ H ₇ (D1), -Ph (E1)	-SH
Group 2	-Ph	Triazole	-H (A2), -CH ₃ (B2), -C ₂ H ₅ (C2), -C ₃ H ₇ (D2), -Ph (E2)	-H
Group 3	-Ph	Triazole	-H (A3), -CH ₃ (B3), -C ₂ H ₅ (C3), -C ₃ H ₇ (D3), -Ph (E3)	-OH
Group 4	-Ph	Triazole	-H (A4), -CH ₃ (B4), -C ₂ H ₅ (C4), -C ₃ H ₇ (D4), -Ph (E4)	-Ph
Group 5	-Ph	Triazole	-H (A5), -CH ₃ (B5), -C ₂ H ₅ (C5), -C ₃ H ₇ (D5), -Ph (E5)	-CN
Group 6	-Ph	Triazole	-H (A6), -CH ₃ (B6), -C ₂ H ₅ (C6), -C ₃ H ₇ (D5), -Ph (E5)	-CH=CH-CN
Group 7	-Ph	Triazole	-H (A7), -CH ₃ (B7), -C ₂ H ₅ (C7), -C ₃ H ₇ (D5), -Ph (E5)	
Group 8	-Ph	Triazole	 (A8)	

* Group 1 is the existing inhibitors, group 2~8 are the new designed homologous inhibitors

Table 7. Quantum chemical parameters and prediction of inhibition efficiency for homologous inhibitors

Group/inhibitor	HOMO/ eV	LUMO/ eV	ΔE / eV	Prediction of inhibition efficiency ^a			Average η	
				(5)	(7)	(8)		
2	A2	-6.865	-2.092	-4.773	84.23	83.68	83.95	83.95
	B2	-6.827	-2.041	-4.785	85.38	84.25	83.60	84.41
	C2	-6.849	-2.045	-4.804	84.69	83.60	83.08	83.79
	D2	-6.816	-2.033	-4.783	85.71	84.48	83.67	84.62
	E2	-6.695	-2.097	-4.598	89.39	88.92	88.79	89.04
3	A3	-6.717	-2.113	-4.604	88.72	88.44	88.63	88.60
	B3	-6.673	-2.031	-4.641	90.06	88.83	87.59	88.83
	C3	-6.664	-2.031	-4.633	90.33	89.09	87.81	89.08
	D3	-6.657	-2.027	-4.630	90.54	89.25	87.89	89.23
	E3	-6.553	-2.146	-4.407	93.68	93.80	94.06	93.85
4	A4	-6.695	-2.097	-4.598	89.39	88.92	88.79	89.03
	B4	-6.598	-2.061	-4.538	92.32	91.44	90.46	91.40
	C4	-6.587	-2.069	-4.518	92.65	91.87	91.00	91.84
	D4	-6.590	-2.066	-4.525	92.57	91.74	90.82	91.71
	E4	-6.457	-2.095	-4.362	96.63	96.15	95.31	96.03
5	A5	-6.975	-2.420	-4.555	80.87	84.34	89.98	85.06
	B5	-6.993	-2.310	-4.683	80.33	82.50	86.44	83.09
	C5	-6.996	-2.301	-4.695	80.23	82.29	86.10	82.87
	D5	-7.014	-2.297	-4.717	79.70	81.71	85.50	82.30
	E5	-6.873	-2.354	-4.519	83.98	86.68	90.98	87.21
6	A6	-6.874	-2.521	-4.353	83.94	88.61	95.57	89.37
	B6	-6.826	-2.381	-4.445	85.42	88.43	93.02	88.96
	C6	-6.813	-2.363	-4.450	85.81	88.61	92.88	89.10
	D6	-6.803	-2.377	-4.427	86.10	89.06	93.53	89.56
	E6	-6.592	-2.428	-4.165	92.51	96.10	100.78	96.46
7	A7	-6.347	-2.127	-4.220	99.95	100.01	99.24	99.73
	B7	-6.330	-2.066	-4.264	100.46	99.81	98.02	99.43
	C7	-6.325	-2.060	-4.265	100.62	99.90	98.00	99.51
	D7	-6.340	-2.095	-4.245	100.18	99.87	98.56	99.54
	E7	-6.320	-2.063	-4.257	100.77	100.08	98.21	99.69
8	A8	-6.070	-2.040	-4.029	108.38	107.30	104.52	106.73

^a Equations (5), (7) and (8) presented in Table 3.

By quantum chemical study, not only can one understand the mechanism of corrosion and inhibitor adsorption on metal surfaces, and determine the merits of corrosion inhibitors, but also the results can help to predict the performance of some homologous corrosion inhibitors, and to provide useful information for the synthesis of these new homologous corrosion inhibitors. According to the quantum properties of the correlation between the chemical parameters and inhibitor performances, performance is good when the main structure of triazole corrosion inhibitors contain R1 (benzene) and R2 (triazole) rings. Hence, we propose other groups of homologous triazole corrosion inhibitors by simply changing R3 and R4 (Table 6, group 2~8), calculate their quantum chemical parameters using B3LYP/6-31+G (d,p) method, and then predict their inhibition efficiency (Table 7) using the formula (5), (7) and (8) (presented in Table 3).

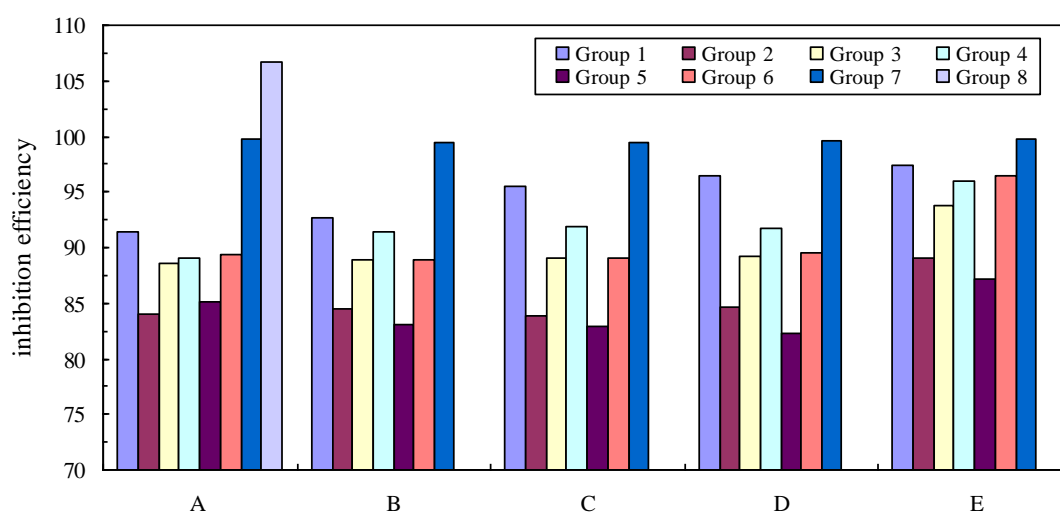


Figure 4. Comparison charts for eight groups of homologous inhibitors and their predicted inhibition efficiencies

Table 7 and Fig.4 provide information about the predicted performance of each inhibitor. If R3 and R4 are better able to donate electron density, the triazole ring R2 will become more negative which could benefit adsorption on the iron surface and potentially better inhibition. As for group 7, R4 is the heteroatomic imidazoliny ring, so the two N atoms may supply more electrons and the R4 ring could also be adsorbed in a parallel arrangement. Therefore, the molecules of group 7 are predicted to have improved corrosion inhibition performance. In addition, if R3 were replaced by imidazoliny as well (group 8), the efficiency may be further improved. After calculation, the HOMO and LUMO energy were obtained: -6.0695 eV and -2.0403 eV, and the average prediction of inhibition efficiency is equal to 106.8%. Though this value greater than 100%, indicates that when R3 and R4 are the same imidazoliny substituents, this inhibitor molecule can get good corrosion performance.

It can be seen from Fig.5 that the optimized inhibitor molecule has a flat shape, and the N atoms of R3 and R4 have more negative charge. Moreover, molecular electrostatic potential surface shows that the negative charge distribution is much more uniform than those in Fig.3. All these factors help this inhibitor to adsorb on metal surface, improving its inhibition effect.

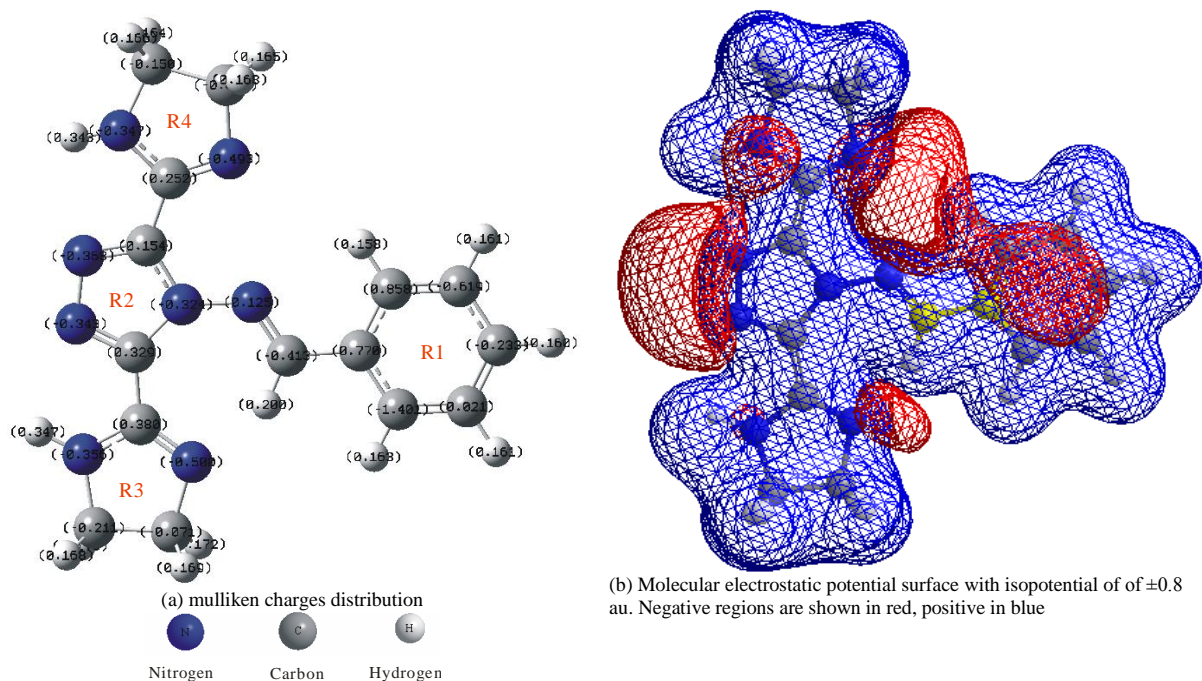


Figure 5. The structure of new inhibitor molecular (R3=R4= imidazoliny)

In order to synthesize these new inhibitors, we design the following reasonable synthetic pathways (Fig.6). By analyzing the reaction pathway, we find there are five steps, in which step (c) will form a transition state (V), so may control the entire reaction. Further studies of thermodynamics and kinetics should be considered. For these calculations, we will further discuss in later research.

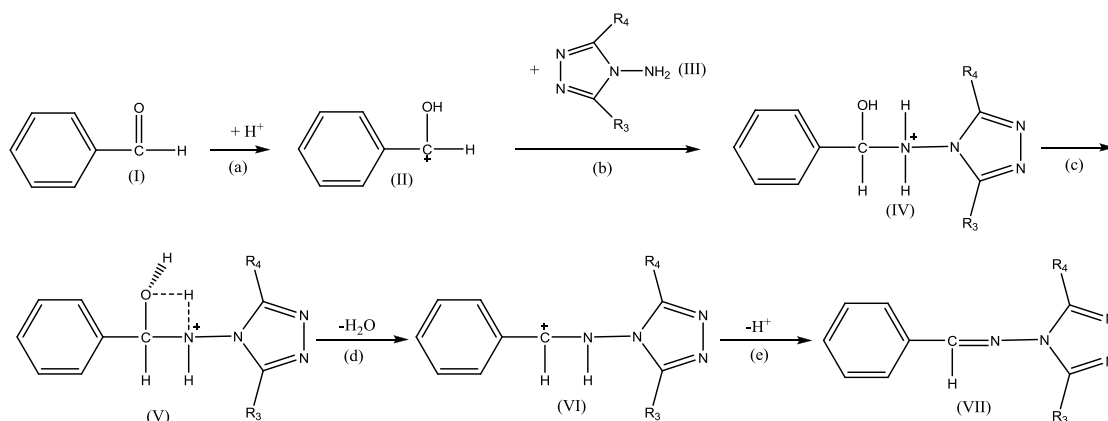


Figure 6. Possible reaction pathways to synthesize these homologous inhibitors

4. CONCLUSIONS

Using quantum chemistry calculation, we have investigated the relationship between corrosion inhibition performance of five benzimidazole inhibitors and their quantum chemical parameters. The detailed studies reveal that corrosion inhibition efficiency and frontier orbital energy level E_{HOMO}

show close correlation. The corrosion inhibition performances of mercapto-triazole inhibitors are mainly decided by E_{HOMO} . The HOMO orbital is mainly delocalized around the triazole ring. Corrosion inhibition efficiency is not closely correlated to net Mulliken charge; NBO charges are not much better. But by analyzing the molecular electrostatic potential surfaces for each molecule, it is found that most of the negative potential is concentrated on the triazole ring R2 and a small part on benzene ring R1. R2 plays a main role and R1 plays a synergistic role during the process of inhibitor adsorption on a metal surface. Further investigation indicates that the interaction energies between corrosion inhibitors and Fe(100) are positively correlated with corrosion inhibition efficiencies. It is theoretically predicted that the main structure of the inhibitor (rings R2 and R1) plays an important role for these inhibitors, as does the HOMO energy. Based on this information, we have attempted to design some superior homologous corrosion inhibitors. It is hoped that testing will reveal the improved performance of these proposed molecules.

References

1. J.Sinko, *Prog. Org. Coat.* 42(2001) 267-282
2. J.Cruz, L.M.Aguilera, R.Salcedo, *Int. J. Quantum. Chem.* 85 (2001) 546-556
3. G.Gece, S.Bilgiç, *Corros. Sci.* 52 (2010) 3435-3443
4. C. Varalakshmi, B. V. Appa Rao, *Anti Corros. Methods Mater.* 48 (2001)171-180
5. B. Fouad, T. Michel, G. Léon, *Appl. Surf. Sci.* 152 (1999) 237-249
6. W.H. Li, H. Qiao, C.L. Pei, *Electrochim. Acta.* 52(2007) 6386-6394
7. M. Lebrini, M. Traisnel, M. Lagrenée, B. Mernari, *Corros. Sci.* 50 (2008) 473-479
8. F. Bentiss, M. Bouanis, B. Mernari, M. Traisnel, *Appl. Surf. Sci.* 253 (2007) 3696-3704
9. N. K. Allam, *Appl. Surf. Sci.* 253 (2007) 4570-4577
10. S.K. Chen, T. Kar, *Int. J. Electrochem. Sci.*, 7 (2012) 6265-6275
11. J. Bartley, N. Huynh, S. E. Bottle, H. Flitt, T. Notoya, D.P Schweinsberg, *Corros. Sci.* 45(2003) 81-96
12. M. A. Quraishi, S. Ahmad, M. Q. Ansari, *Br. Corros. J.* 32 (1997)297-300
13. M. A. Quraishi, D. Jamal (2001) *Mater Chem. Phys.* 68: 283-287
14. F. Bentiss, M. Lagrenée, M. Traisnel, J. C. Hornez, *Corros. Sci.* 41 (1999)789-803
15. G. Gece, *Corros. Sci.* 50 (2008) 2981-2992
16. L. M. Rodriguez-Valdez, A. Martinez-Villafane, D. Glossman-Mitnik, *J. Mol. Struct. – THEOCHEM* 10 (2005) 65-70
17. S. Affrossman, J. Daviot, D. Holmes, R. A. Pethrick, M. Wilson, *Corros. Sci.* 43 (2001) 939-950
18. K. F. Khaled, *Electrochim. Acta.* 53 (2008) 3484-3492
19. Y. Duda, R. Govea-Rueda, M. Galicia, H. I. Beltrán, L. S. Zamudio-Rivera, *J. Phys. Chem. B* 109(2005) 22674-22684
20. J. Hong, Z. P. Kai, L. Yan, *Corros. Sci.* 50(2008) 865-871
21. M. Şahin, S. Bilgiç, H. Yılmaz, *Appl. Surf. Sci.* 195(2002) 1-7
22. G. Gece, S. Bilgiç, *Corros. Sci.* 51 (2009) 1876-1878
23. M. Hosseini, S. F. L. Mertens, M. Ghorbani, M. R. Arshadi, *Mater. Chem. Phys.* 78 (2003) 800-808
24. K. F. Khaled, *Corros. Sci.* 52(2010)2905-2916
25. I. B. Obot, N. O. Obi-Egbedi, *Corros. Sci.* 52 (2010)282-285
26. J. Zhang, G. M. Qiao, S. Q. Hu, Y. G. Yan, Z. J. Ren, L. J. Yu, *Corros. Sci.* 53 (2011)147-152
27. K. F. Khaled, S. A. Fadel-Allah, B. Hammoutic, *Mater. Chem. Phys.* 117 (2009).148-155

28. T. Arslan, F. Kandemirli, E. E. Ebenso, I. Love, H. Alemu, *Corros. Sci.* 51 (2009) 35-47
29. L. B. Tang, X. M. Li, L. Lin, G. N. Mu, G. H. Liu, *Surf. Coat. Technol.* 201(2006) 384-388
30. F. Touhami, A. Aouniti, Y. Abed, B. Hammouti, S. Kertit, A. Ramdani, K. Elkacemi, *Corros. Sci.* 42(2000) 929-940
31. P. Hohenberg, W. Kohn, *Phys. Rev.* 136(1964)B864-B871
32. W. Kohn, L. J. Sham, *Phys. Rev.* 140 (1965)A1133-A1138
33. M. J. Frisch, G. W. Trucks, H. B. Schlegel, Gaussian, revision B 09 Pittsburgh, Pa: Gaussian Inc, 2009
34. M. Ozcan, I. Dehri, *Progr. Org. Coat.* 51 (2004)181-187
35. M. Lebrini, M. Lagrenée, H. Vezin, M. Traisnel, F. Bentiss, *Corros. Sci.* 49(2007) 2254-2269
36. A. V. Marenich, C. J. Cramer, D. G. Truhlar, *J. Phys. Chem. B* 113 (2009) 6378-6796
37. H. L. Wang, R. B. Liu, J. Xin, *Corros. Sci.* 46 (2004)2455-2466
38. H. L. Wang, R. B. Liu, J. Xin, *Chem. Res.* 15 (2004)58-61 (In Chinese)
39. P. Dauber-Osguthorpe, V. A. Roberts, D. J. Osguthorpe, J. Wolff, M. Genest, A. T. Hagler, *Proteins: Struct. Function Genetics* 4 (1988) 31-47
40. Y. M. Tang, X. Y. Yang, W. Z. Yang, Y. Z. Chen, R. Wan, *Corros. Sci.* 52 (2010) 242-249